This article was downloaded by: [Ohio State University Libraries]
On: 23 April 2013, At: 12:31
Publisher: Taylor & Francis
Informa Ltd Registered in England and Wales Registered Number: 1072954 Registered office: Mortimer House, 37-41 Mortimer Street, London W1T 3JH, UK

Particulate Science and Technology: An International Journal
Publication details, including instructions for authors and subscription information:
http://www.tandfonline.com/loi/upst20

Integrated Process for Purification of Low Grade Talc Ores

Luciana A. Castillo [a] , Silvia E. Barbosa [a] , Pedro Maiza [b] & Numa J. Capiati [a]
[a] Planta Piloto de Ingenieria Quimica (UNS - CONICET) Camino La Carrindanga Km. 7
[b] Dpto. de Geologia - UNS, Bahía Blanca, Argentina

Accepted author version posted online: 21 Dec 2012.

To cite this article: Luciana A. Castillo , Silvia E. Barbosa , Pedro Maiza & Numa J. Capiati (2012): Integrated Process for Purification of Low Grade Talc Ores, Particulate Science and Technology: An International Journal, DOI:10.1080/02726351.2012.755588

To link to this article: http://dx.doi.org/10.1080/02726351.2012.755588

Disclaimer: This is a version of an unedited manuscript that has been accepted for publication. As a service to authors and researchers we are providing this version of the accepted manuscript (AM). Copyediting, typesetting, and review of the resulting proof will be undertaken on this manuscript before final publication of the Version of Record (VoR). During production and pre-press, errors may be discovered which could affect the content, and all legal disclaimers that apply to the journal relate to this version also.

PLEASE SCROLL DOWN FOR ARTICLE

Full terms and conditions of use: http://www.tandfonline.com/page/terms-and-conditions

This article may be used for research, teaching, and private study purposes. Any substantial or systematic reproduction, redistribution, reselling, loan, sub-licensing, systematic supply, or distribution in any form to anyone is expressly forbidden.

The publisher does not give any warranty express or implied or make any representation that the contents will be complete or accurate or up to date. The accuracy of any instructions, formulae, and drug doses should be independently verified with primary sources. The publisher shall not be liable for any loss, actions, claims, proceedings, demand, or costs or damages whatsoever or howsoever caused arising directly or indirectly in connection with or arising out of the use of this material.

Integrated Process for Purification of Low Grade Talc Ores

Luciana A. Castillo[1], Silvia E. Barbosa[1], Pedro Maiza[2], Numa J. Capiati[1]

[1]Planta Piloto de Ingenieria Quimica (UNS - CONICET) Camino La Carrindanga Km. 7,
[2]Dpto. de Geologia – UNS, Bahía Blanca, Argentina

Address correspondence to Silvia E. Barbosa, Planta Piloto de Ingenieria Quimica (UNS–CONICET) Camino La Carrindanga Km. 7, 8000), Bahía Blanca, Argentina Email: sbarbosa@plapiqui.edu.ar

Abstract

This study examines the development of an integrated process for separation and purification of low grade talc ores. This procedure involves leaching with HCl to dissolve gangue minerals and to purify a low purity talc ore containing up to 40% gangue minerals. Also, all cations from gangue minerals are recovered as hydroxides via selective precipitation. The effects of acid concentration, talc/acid solution ratio, time, and reaction temperature on talc purification were studied and the optimal conditions were determined. Laboratory-scale tests revealed that the resulting talc is free of gangue minerals, consisting of small particles with nanometric thicknesses. Reactants are fully consumed during dissolution and byproducts like ammonium chloride could be recirculated and reused. Resulting hydroxides can be used as a coagulation aid for water treatment.

KEYWORDS: talc; purification; carbonates; chlorite; recovery; acid treatment.

1. INTRODUCTION

The world production of commercial talc and pyrophyllite has reached an important level of about 7.5 million tons/year, placing it as a promising mineral commodity worthy of upgrading (Virta, 2006). Nowadays, industrial quality talc finds many applications in paint, paper, plastics, rubbers, fertilizers, insecticides, while high purity ones are used in ceramics, cosmetics and medical compounds (Okunkola et al., 2003; Ferrage et al., 2003a; Ferrage et al., 2003b; Chandra et al., 2004; Helmy et al., 2005).

Talc contains different associated minerals and impurities depending on its ore. This characteristic determines talc quality and consequently its possible market. Associated minerals generally include carbonates, like dolomite ($CaMg(CO_3)_2$), calcite ($CaCO_3$), and magnesite ($MgCO_3$); as well as chlorite ($Mg_5(Al,Fe)(Al,Si)_4O_{10}(OH)_8$) and serpentine (Boghdady et al., 2005). In Argentina, main talc deposits are situated on the foothills of Andean mountains range, mostly in Mendoza and San Juan provinces. However, as it is associated mainly with calcium and magnesium carbonates and iron-aluminum silicates in a considerable proportion, it does not fill the specific requirements for applications like paints, plastics, medicine, cosmetics, etc (Castro, 1996). Associated minerals form macroscopic particles whose structure is not strictly laminar, therefore more difficult to disaggregate (Clark and Steen, 2003; Lozano and Bernal, 2005). Generally speaking, Argentinean talc contains up to 40 wt% of carbonates. Taking into account that the estimated talc reserves are approximately 2.000.000 tons (Castro, 1996), recovery of either talc or associated minerals is an important economic field to explore. In this sense, several methods were probed. Flotation is the preferred concentration technique to remove impurities from talc due to its low cost (Yehia and Al-Wakeeel, 2000; Boulos, 2004). This method was applied by Amehd et al. (2007) to upgrade Egyptian talc quality having less than 13% of impurities up to reach industrial quality standards. Their results show that in spite of talc quality improvement, complete extraction of iron and aluminum was not possible by this technique. To solve iron extraction problems, flotation was combined with magnetic separation, obtaining improved results (Piga and Maruzzo, 1992; Houot et al., 1995; Al-Wakeeel, 1996; Boulos, 2004). However, this technique is not effective for purifying Argentinean talc because gangue minerals are not separated adequately from talc flakes, as a consequence of their paragenesis, which is different from Egyptian talc. Other authors suggested that sonication treatments helped to talc delamination and particle size reduction (Feng and Aldrich, 2004; Perez-Maqueda et al., 2005; Jamil and Palaniandy, 2010). However, this technique applied on talc containing a considerable amount of associated minerals, is not possible for the same reasons explained above. Also, it is not directly applicable to industrial processes because of its high cost (Feng and Aldrich, 2004; Jaramillo et al., 2005; Perez-Maqueda et al., 2005; Ahmed et al., 2007).

Jaramillo et al. (2005) have reported that acid leaching was more effective than froth flotation to remove iron oxides from talc, mainly by dissolution. However, acid attack could also affect the crystal structure of mineral due to the dissolution of structural ions and/or the rearrangement of its structure (Temuujin et al., 2002). Consequently, this technique is attractive only if host mineral is relatively inert to acids or for obtaining porous material (Yang et al., 2006).

The reaction of associated minerals during acid leaching of low grade talc is favored with respect to talc dissolution, mainly by the different reactivities. This claim is based on the fact that the major impurities are carbonates like calcite, magnesite, and dolomite, which react with acid. Carbonates are dissolved releasing their soluble cations, water and carbon dioxide. Carbonates have different acid reactivities and therefore the reaction conditions must be selected in order to solubilize all of them. These reactions are competitive and faster than acid dissolution of talc as it contains a large number of SiO_4 tetrahedral groups (Harben, 1992). Consequently, talc structure from ores with large amounts of impurities will be less affected yielding a purified material with similar crystal order to the initial mineral.

The direct action of acid on talc ores would result in purified talc (solid phase), pure collectable CO_2, , and a liquid acid solution containing all of cations present in the associated minerals. From this solution, hydroxides of the soluble cations can be obtained by sequential treatment. Taking into account the differences in solubility product constant (K_{sp}) of hydroxides and the influence of pH and temperature on K_{sp}, it is possible to obtain relative pure hydroxides by an appropriated selection and control of process conditions (Christian, 1986).

In the present work, a whole process to purify low grade talc ore is proposed. This procedure allows recovering, by a selective precipitation, cations from dissolved gangue minerals as hydroxides. This process involves controlled acid treatment that could be used for ores containing up to 40% of gangue minerals. It also contributes to environmental preservation since byproducts can either be reused in the same process or have commercial value, avoiding their disposal.

2. EXPERIMENTAL

2.1. Material

Talc ore samples from San Juan province (Argentina) with different gangue content and particle size were kindly supplied by Dolomita SAIC. Table 1 shows nominal particle size and associated minerals percentage in the studied samples provided by the supplier. In the same table, sample denomination is also listed. High purity hydrochloric acid (HCl) from Merck was used for acid leaching. Ammonium hydroxide (NH_4OH) 28% from Anedra, and high purity ammonium chloride (NH_4Cl) were used as precipitation precursors.

2.2. Purification Process

The flow sheet of the proposed process for talc purification and associated minerals recovery is shown in Fig. 1. The process includes dissolution of associated minerals by direct contact of talc powder with concentrated HCl in a stirred vessel. Trial experiments were performed in order to assess the optimal operating conditions. The reaction was carried out at 60 and 80°C, with acid concentration varying from 1.7 to 12 M. Talc/acid solution ratio was defined as the mass of mineral subjected to extraction per volume unit of acid solution. Three talc/acid solution ratios were tested: 100, 250 and 300 $g_{talc}/L_{acid\ solution}$. The minimum time needed to complete the minerals dissolution (30 min) was estimated from the disappearance of CO_2 bubbles in the reacting media. In this sense, three reaction times were used in the experiments 30, 60, and 120 min. Once solid phase was washed and dried, it resulted in purified talc. The amount of associated minerals corresponding to the extracted mass in each sample was determined by gravimetric methods, being samples weighed before and after each treatment up to constant weight.

The recovery of cations in the supernatant acid was obtained by selective precipitation through controlled pH increases. Initially, pH was adjusted to 5 with concentrated NH_4OH using a buffer solution of NH_3/NH_4Cl in order to separate Fe hydroxides. Then, pH was increased to 12 to precipitate a mixture of Ca and Mg hydroxides. The remaining supernatant contains only NH_4Cl, which was recovered by evaporation of water.

2.3. Characterization

Mineral samples were characterized before and after acid leaching with X-ray Diffraction (XRD) using a Rigaku DMAX III C difractometer at 35 kV and 15 mA, CuKα and graphite monocromator in 2θ ranged 3 to 60°.

Mineral composition of initial and purified talcs was also analyzed by Fourier Transform Infrared Spectroscopy (FTIR). A Nicolet 520 FTIR spectrophotometer was used. Spectra were obtained in the range from 400 to 4000 cm^{-1}, running 100 scans at a resolution of 4 cm^{-1}. Samples were diluted to 3% in potassium bromide (KBr). Thermogravimetric Analysis (TGA) was applied to quantify the amount of different mineral species. A Perkin Elmer TGS-2 balance was used, heating samples from 25 to 1000°C under nitrogen gas atmosphere with a heating rate of 20°C/min.

Optical Microscopy (OM) was employed to identify the presence of associated minerals and their distribution in talc ore. This analysis was performed on thin sections of the mineral with transmission polarized light in a Leica DFC 280 microscope. Particle morphology was observed by Scanning Electron Microscopy (SEM) in a JEOL 35 CF microscope equipped with an energy dispersive X-ray (EDS) microanalyzer. The effects of acid treatment on particle size reduction were observed in greater detail by Transmission Electron Microscopy (TEM) in a JEOL 100 CX TEM at 100 kV. Talc samples were embedded in a resin and then sectioned in a Leica Ultracryomicrotome.

The cations present in the supernatant liquid after acid leaching were determined with various analytical techniques. Initially, elements were identified by X-ray Fluorescence using a PANalytical MagiX XRF spectrometer. Data were processed with SuperQ software. Iron was quantified by molecular absorption spectrophotometry (UV-visible) in a Shimadzu UV-1601 instrument, using the potassium thiocyanate technique (Slowinski and Wolsey, 2009). Calcium, magnesium, aluminium, and silicon were assessed by Atomic Absorption Spectrophotometry (AAS) with a Perkin Elmer Aanalyst 200 spectrophotometer. The same experimental routine was applied on the precipitates.

3. RESULTS AND DISCUSSION

3.1. Talc Ore

Thermogravimetrical analysis was used to confirm the nominal gangue content of initial talc samples and to identify the gangue mineral species. Fig. 2a shows TGA curves for T1 and T3 talc samples. Supplier data of gangue percentage in each sample (see Table 1) were corroborated. In TGA thermograms, peaks were assigned to magnesite, dolomite, calcite, and chlorite, based on literature data (Gallagher, 2003). In order to confirm the kind of minerals in gangue, XRD and FTIR analyses were performed. XRD spectrum (Fig. 2b) confirms that associated minerals in all samples are magnesite, dolomite, calcite, and chlorite. Different species are identified with a capital letter in the figure, following the literature database. FTIR spectrum in Fig. 2c also corroborates the gangue mineral species in talc ore. Except for typical talc bands (υMg2Fe-OH at 3660 cm^{-1}, υSi-O-Si at 1010 and δOH at 660 cm^{-1}); dolomite and calcite (2520, 1440 and 878 cm^{-1}), as well as magnesite (at 744 cm^{-1}) are present (Van der Marel and Beutelspacher, 1976).

SEM micrographs in Fig. 3 show the morphology of talc particles and EDS spectra from T1 and T3 samples. The overall particle morphology includes blocky layers reduced to irregularly faceted blocks having similar lengths in all directions, smooth faces and very acute angles (Ferrage et al., 2002). Particle morphology also reveals the macrocrystalline character of this talc (Clark and Steen, 2003). In addition, trigonal geometry and rhombohedral cleavage, typical crystalline habits corresponding to carbonates are also visible in Fig. 3c (Gamiz et al., 2002). Chlorite crystals are flatter and thicker cleaved laminates. From EDS spectra (Figs. 3a and 3b), the presence of C, Fe, and Ca is confirmed, besides Si, Mg, and O. Although it is known that chlorite generally contains Al, this element was not detected in EDS spectrum, probably because its low concentration under the limit of equipment detection.

Associated minerals in talc ore are shown in Fig. 4. Argentinean talc contains lenticular veins associated with carbonates and chlorite. These characteristics are mainly determined by geological evolution of the deposit regarding Argentinean talc deposits

(Bjerg et al., 1999; Kostadinoff et al., 2004). Gregori and Mercader (1994) determined the composition of some Argentinean chlorites by using Mossbauer Spectroscopy assessing high Fe content in accordance with our results. Also, they also explain that iron can replace both Mg and Al in crystal structure in a fraction and site that depending on the mineral thermal and chemical histories.

3.2. Products From Proposed Process

3.2.1. Purified Talc

The effectiveness of the proposed process on talc is evaluated in terms of purity degree and particle size. In this sense, the extracted mass for each sample at several experimental conditions were tested in order to select the optimal ones for the purification process. The analyzed variables were acid concentration, talc/acid solution ratio, time, and temperature.

Effect of the acid concentration: Four different acid concentrations were used ranging from 1.7 to 12 M. The extracted mass for each particle size, using talc/acid solution ratio of 100 $g_{talc}/L_{acid\ solution}$ at 80°C for 120 min is presented in Fig. 5a. There is no variation in the extracted mass with acid molarity in this range as HCl is a so strong acid even at the low concentration tested (1.7 M).

Effect of talc/acid solution ratio: Acid leaching of samples with different talc particle size using 1.7 M HCl at 80°C for 120 min was tested by varying talc/acid solution ratio from 100 to 333 $g_{talc}/L_{acid\ solution}$. Fig. 5b shows that talc/acid solution ratio is not an important variable in the studied range. This parameter is associated mainly with providing enough acid for talc leaching and with suspension diffusion and hydrodynamics.

Effect of leaching time: The effect of the reaction time was evaluated in batch experiments within the range 30-120 min, with 1.7 M HCl, using a talc/acid solution ratio of 100 $g_{talc}/L_{acid\ solution}$ and at 80°C. Dissolution of impurities is not completed after 30 min for any particle size (Fig. 5c). However, as time increases dissolution is completed. For larger particle size and associated minerals content, complete extraction needs more time, as expected.

Effect of leaching temperature: This is the variable that affects gangue minerals dissolution to a greater extent. Complete dissolution requires at least 80°C using 1.7 M HCl, a talc/acid solution ratio of 100 $g_{talc}/L_{acid\ solution}$, and 120 min reaction time (Fig. 5d). This result agrees with the fact that mineral dissolution is a thermally activated phenomenon; thus, rates increases as a function of temperature (Lund et al., 1973).

Taking into account all these results, the optimal conditions for purification are acid concentration 1.7 M HCl, talc/acid solution ratio 100 $g_{talc}/_{Lacid\ solution}$, reaction time 120 min and temperature 80°C. In the studied talc samples, particle size and impurity contents are interrelated due to milling and separation processes.

The resulting purified talc was characterized quantitatively and qualitatively in order to assess its purity. In this way, a comparative analysis between purified and untreated talc was performed using XRD, TGA, FTIR, EDS, SEM, and TEM. Fig. 6 shows the X-ray diffractogram of purified talc. This sample does not exhibit the characteristic peaks of gangue minerals present in the initial one (Fig. 2b). A slight talc dissolution is observed when the full with at half maximum (FWHM) of (001) talc peak is compared between initial and purified samples. FWHM values of treated talc samples are around 10% higher than corresponding to initial ones indicating a less crystal ordering.

Fig. 7 shows the derivative weight curve data from DTG of initial and purified talc samples. Disolution of dolomite, calcite, magnesite, and chlorite by HCl is evident because their corresponding peaks are absent. Regarding talc dissolution, only a little variation in talc mass loss is observed by comparing DTG curves of initial and purified talc, agreeing with the conclusions obtained from XRD data.

The final quality of purified talc was also corroborated by FTIR (Fig. 8) where only typical bands of talc are present. Please compare the spectra of Fig. 2c (initial talc) with Fig. 8 (purified talc). Ulterior confirmation of the high purity degree obtained by the proposed process is provided by EDS spectra of treated talc in Fig. 9. The absence of impurities containing C, Ca and Fe gives an independent confirmation of the results presented and discussed above.

In order to estimate the effect of acid treatment on final particle size (length and thickness), electronic microscopy techniques were used. SEM micrographs from untreated and treated talcs, included in Fig. 9, show net changes in overall particle dimensions. Treated talc particles consist of thin layers (in the nanometric range) having micrometric scale in the other two dimensions. Considerable delamination is observed in Fig. 9, particularly by comparing to the micrographs in Fig. 4, which shows the intercalated structure where thin veins of carbonates and chlorite intergrowth among talc flakes. This last claim is corroborated by TEM micrographs (Fig. 10) where nanometric thicknesses observed in final particles are more evident. These results illustrate that high level of talc purification and particle size reduction can be attained by acid leaching of low grade talc.

3.2.2. Associated Minerals Recovery

The supernatant liquid after HCl treatment exhibits an intense yellow color, typical of acid solutions containing Fe^{3+}. Table 2 lists the concentration of Ca^{2+}, Mg^{2+}, Fe^{3+}, Al^{3+}, and Si^{4+} in this acid supernatant obtained in the aforementioned experimental conditions. The concentration of Mg^{2+} is relative higher than Ca^{2+}, and Fe^{3+} one, in accordance with the content and type of gangue minerals identified above. Low detected Al^{3+} concentration is compatible with the fact that chlorite contains low Al content and high Fe one, agreeing with EDS analysis on initial talc and with previous results (Gregori and Mercader, 1994). In Table 2, only traces of Si are present. This result is in agreement with the low level of talc dissolution.

The procedure described above in Fig. 1 was followed in order to separate and recover the cations from the acid solution. At pH 5, iron precipitates as brownish red floccules of ferric hydroxide, which can be easily separated from the solution. Table 3 shows the corresponding X-ray fluorescence data from the precipitated obtained during cation recovery. The analysis of the brownish precipitate showed Fe as main element along with traces of Ca, Mg, Si, and Al. Please note that the proposed process could be used also with chlorites with relative high content of Al. In this case, Al will precipitate as $Al(OH)_3$ at similar pH than $Fe(OH)_3$. This claim is based on the values of solubility product constant at 25°C ($K_{sp\ Fe(OH)3}$= 4.0 10^{-38}, $K_{sp\ Al(OH)3}$=4.6 10^{-33}).

The residual transparent supernatant did not contain Fe, as it was checked by AAS. It contains $Ca^{2+,}$ Mg^{2+} and $NH_4{}^{1+}$ ions to be isolated and recovered. At pH 12, Mg and Ca hydroxides precipitate as white floccules. By X-ray Fluorescence, Mg and Ca were detected (Table 3). Also, traces of Si and Al were found. The remaining supernatant is essentially an aqueous solution of NH_4Cl, which can be reused as component of the buffer solution, when crystallizes after evaporation of excess water (Somasundaran and Liu, 1995).

4. CONCLUSIONS

An integrated process for purifying low grade talc ores is proposed which yields highly purified talc maintaining its morphological characteristics. The method improves delamination of talc,obtaining nanometric thickness particles. This result seems to be independent of the initial particle size. Also, this procedure involving selective precipitation allows recovering cations from dissolved gangue minerals as hydroxides, giving them more added values. The process was tested with talc ores containing gangue minerals up to 40% in weight with good results.

The proposed procedure would present low ecological risk because it minimizes byproducts. Although it uses high concentration acids, these are fully consumed during the process. Byproducts like ammonium chloride could be recirculated and reused in the same process. Also, “acidic” water could be neutralized by the process products (hydroxides), improving its disposal.

REFERENCES

Ahmed, M.M., Ibrahim, G.A., Hassan, M. 2007. Improvement of Egyptian talc quality for industrial uses by flotation process and leaching. *Int. J. Miner. Process.* 83: 132-145.

Al-Wakeeel, M.I. 1996. Geology and beneficiation of some Egyptian talc– carbonate rocks. *PhD Dissertation*. Ain Shams University, Egypt.

Bjerg, E., Villar, L., Donnari, E. 1999. Distrito Cuprifero Salamanca, Complejos Novillo Muerto y Los Gateados, Mendoza. In: *Recursos Minerales de la República Argentina*, ed. E. Zappettini. Instituto de Geologia y Recursos Minerales, SEGEMAR, Argentina, pp. 167-174.

Boghdady, G., Ahmed, M., Ibrahim, G., Hassan, M. 2005. Petrographical and geochemical characterisation of some Egyptian talc samples for possible industrial applications. *J. Eng. Sci.* 33: 1001-1011.

Boulos, T.R. 2004. Transforming upgrading of talc for different industrial application. Final Report. Egyptian Academy for Scientific Research and Technology.

Castro, G.A. 1996. Diagnostico de la produccion de talco frente a la demanda en Argentina. *Información Tecnológica* 7 (4): 175-181.

Chandra, N., Agnihotri, N., Bhasin, S. 2004. Sintering characteristic of talc in the presence of phosphates and alkali carbonate sintering activators. *Ceram. Int.* 30: 643-652.

Christian, G.D. 1986. *Analytical chemistry*, fourth ed. New York: John Wiley & Sons.

Clark, R.J., Steen, W.P. 2003. Talc in Polypropylene. In: *Handbook of Polypropylene and Polypropylene Composites,* 2nd Edition. Ed. by H.G. Karian. USA: RheTech Inc. pp. 251-278.

Feng, D., Aldrich, C. 2004. Effect of ultrasonication on the flotation of talc. *Ind. Eng. Chem. Res.* 43: 4422-4427.

Ferrage, E., Martin, F., Boudet, A., Petit, S., Fourty, G., Jouffret, F., Micoud, P., De Parseval, D., Salvi, S., Bourgertee, C., Ferret, J., Saint-Gerard, Y., Buratto, S., Fortune, J. 2002. Talc as nucleating agent of polypropylene: morphology induced by lamellar particles addition and interface mineral matrix modelization. *J. Mater. Sci.* 37: 1561-1573.

Ferrage, E., Martin, F., Petit, S., Pejo-Soucaille, S., Micoud, P., Fourty, G., Ferret, J., Salvi, S., de Parseval, P., Fortune, J. 2003a. Evaluation of talc morphology using FTIR and H/D substitution. *Clay Miner.* 38: 141-150.

Ferrage, E., Martin, F., Micoud, P., Petit, S., de Parseval, P., Beziat, D., Ferret, J. 2003b. Cation site distribution in clinochlores a NIR approach. *Clay Miner.* 38: 329-338.

Gallagher, P.K. 2003. *Handbook of Thermal analysis and calorimetry. Applications to inorganic and Miscellaneous materials.* Volume 2. Brown M. and Gallagher P. (Eds.). Elsevier, Amsterdam.

Gamiz, E., Soriano, M., Delgado, G., Parraga, J., Delgado, R. 2002. Estudio morfologico de talcos con microscopio electronico de barrido (SEM). Aplicaciones farmaceuticas. *Ars Pharmaceutica* 43: 173- 185.

Gregori, D.A., Mercader, R.C. 1994. Mossbauer study of some Argentinean chlorites. Hyperfine *Interact* 83:495-498.

Harben, P. 1992. *The industrial mineral handbook*. London, UK: Metal Bulletin plc.

Helmy, A., Ferreiro, E., de Bussetti, S. 2005. The surface energy of talc. *J. Colloid Interface Sci.* 285:

314-317.

Houot, R., Joussemet, R., Yang, S., Baeza, R. 1995. Beneficiation of talc products, processing of hydrophobic minerals and fine coal. In *Proc. 1st UBC-McGill Bi-Annual International Symposium of Fundamentals in Mineral Processing*. Vancouver, BC, Canada. pp. 373-377.

Jaramillo, L.I., Mesa Restrepo, J.A., Tobon, J.I., 2005. Estudio preliminar de blanqueamiento del talco de la Union (Antioquia). *Dyna* 72: 1-11.

Jamil, N.H., Palaniandy S. 2010. Acid medium sonication: A method for the preparation of low density talc nano-sheets. *Powder Technology* 200: 87-90.

Kostadinoff, J., Bjerg, E., Gregori, D., Richarte, D., Robles, J., Raniolo, A. 2004. Geofisica del cuerpo ultramafico de la mina Salamanca, provincia de Mendoza. *Revista de la Asociación Geológica Argentina* 59: 113-120.

Lozano, R., Bernal, J. 2005. Composicion quimica, clasificacion y caracterizacion de los minerales del grupo de las cloritas. *Boletín de Mineralogía* 16: 1-20.

Lund, K., Fogler, H., McCune, C.C. 1973. Acidization-I. The dissolution of dolomite in hydrochloric acid. *Chemical Engineering Science* 28 (3): 691-700.

Okunkola, O., Ogedengbe, O., Ojutalyo A. 2003. Composition features and industrial appraisal of the Babe Ode talc occurrence southwestern Nigeria. *Global J. Geol. Sci.* 1: 63-72.

Perez-Maqueda, L.A., Duran, A., Perez Rodriguez, J.L. 2005. Preparation of submicron talc particles by sonication. *Appl. Clay Sci.* 28: 245-255.

Piga, L., Marruzzo, G., 1992. Preconcentration of an Italian talc by magnetic separation and attrition. Int. *J. Miner. Process.* 35: 291-297.

Slowinski, E.J., Wolsey, W.C. 2009. *Chemical Principles in the Laboratory*. *Ninth edition*. United States of America: Brooks/Cole, Cengage Learning.

Somasundaran, P., Liu, D. 1995. Dissolved mineral species precipitation during coal flotation. In *Proceedings XIV International Mineral Processing Congress*, San Francisco.

Temuujin, J., Okada, K., Jadambaa, T., Mackenzie K., Amarsanaa J. 2002. Effect of grinding on the preparation of porous material from talc by selective leaching. *J. Mater. Sci. Lett.* 21(20): 1607-1609.

Van der Marel, H.W., Beutelspacher, H. 1976. *Atlas of Infrared Spectroscopy of Clay Minerals and Their Admixtures*. Amsterdam: Elsevier.

Virta, R.L. 2006. *Mineral Commodity Summaries*, Open-File Report, US Geological Survey.

Yang, H., Du, C., Hu, Y., Jin, S., Yang, W., Tang, A., Avvakumov, E.G. 2006. Preparation of porous material from talc by mechanochemical treatment and subsequent leaching. *Appl. Clay Sci.* 31: 290- 297.

Yehia, A., Al-Wakeeel, M.I. 2000. Talc separation from talc–carbonate ore to be suitable for different industrial applications. *Min. Eng.* 13: 111-116.

Table 1. Name, average diameter (d50) and content of associated minerals (supplied by Dolomita SAIC) of talc samples

Talc	d(50) (μm)	Average content of associated minerals* (% wt)
T1	5.9	16.0 ± 1.5
T2	11.5	35.0 ± 0.7
T3	16.5	40.0 ± 1.9

*Determined by Thermogravimetric analysis.

Table 2. Elemental analysis in the acid supernatant.

Element	Concentration [mg/L]
Fe^{3+}	2837.1
Ca^{2+}	2390.0
Mg^{2+}	9016.0

Table 3. X-ray fluorescence ratios (%)* of detected elements from different precipitates.

Detected elements	Brownish precipitate (pH:5)	White precipitate (pH:12)
Fe	57.0	-
Ca	1.2	75.7
Mg	0.25	16.7
Cl	38.8	1.0

* Normalized to the major component in each precipitate

Figure 1

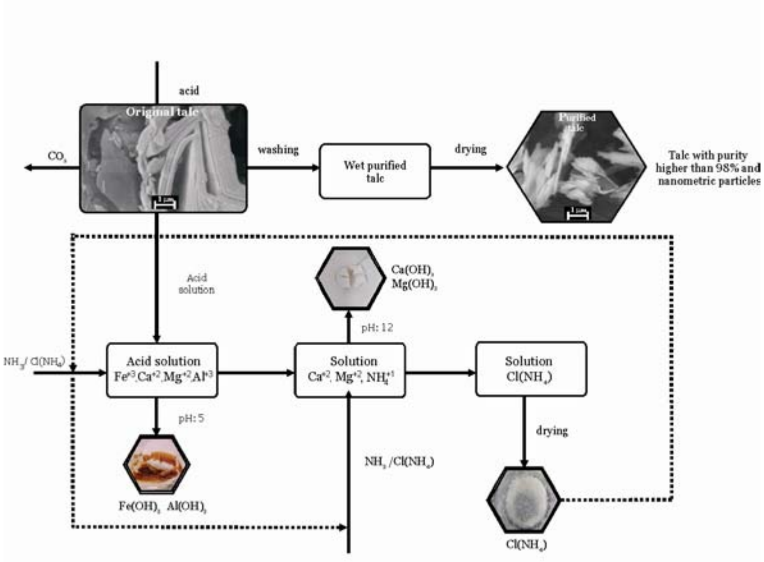
acid
Original talc
CO_2
washing
Wet purified talc
drying
Purified talc
Talc with purity higher than 98% and nanometric particles
Acid solution
$Ca(OH)_2$
$Mg(OH)_2$
pH: 12
NH_3/ $Cl(NH_4)$
Acid solution
Fe^{+3},Ca^{+2},Mg^{+2},Al^{+3}
Solution
Ca^{+2}, Mg^{+2}, NH_4^{+1}
Solution
$Cl(NH_4)$
pH: 5
drying
NH_3 /$Cl(NH_4)$
$Fe(OH)_3$ $Al(OH)_3$
$Cl(NH_4)$

Figure 2

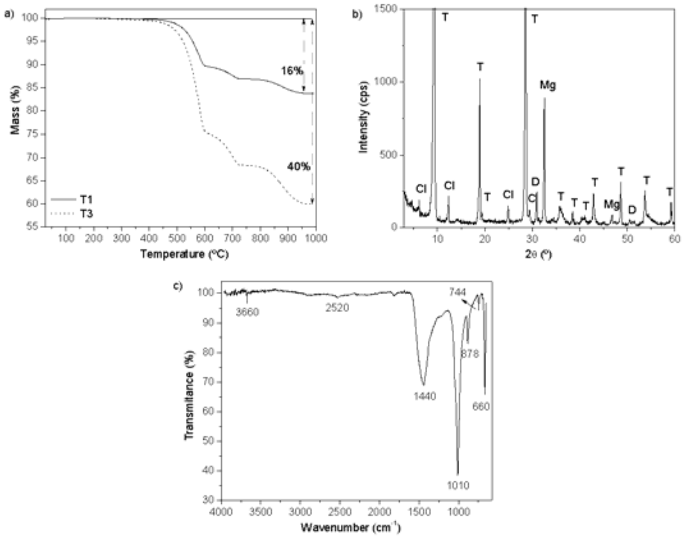
a)
Mass (%)
100
95
90
85
80
75
70
65
60
55
100
200
300
400
500
600
700
800
900
1000
Temperature (ºC)
16%
40%
T1
T3
b)
Intensity (cps)
1500
1000
500
0
10
20
30
40
50
60
2θ (º)
T
T
T
Mg
Cl
Cl
T
Cl
D
C
T
T
T
T
Mg
T
D
T
T
c)
Transmitance (%)
100
90
80
70
60
50
40
30
4000
3500
3000
2500
2000
1500
1000
Wavenumber (cm-1)
3660
2520
744
878
1440
660
1010

Figure 3

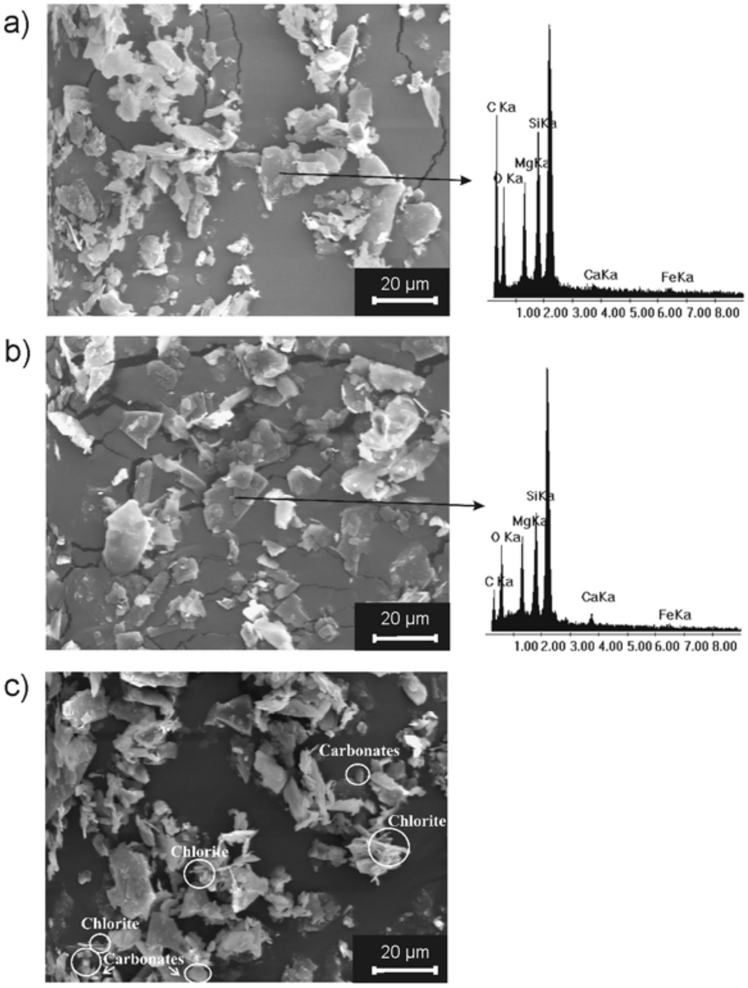
a)
20 µm
C Ka
SiKa
MgKa
O Ka
CaKa
FeKa
1.00 2.00 3.00 4.00 5.00 6.00 7.00 8.00
b)
20 µm
SiKa
MgKa
O Ka
C Ka
CaKa
FeKa
1.00 2.00 3.00 4.00 5.00 6.00 7.00 8.00
c)
Carbonates
Chlorite
Chlorite
Chlorite
Carbonates
20 µm

Figure 4

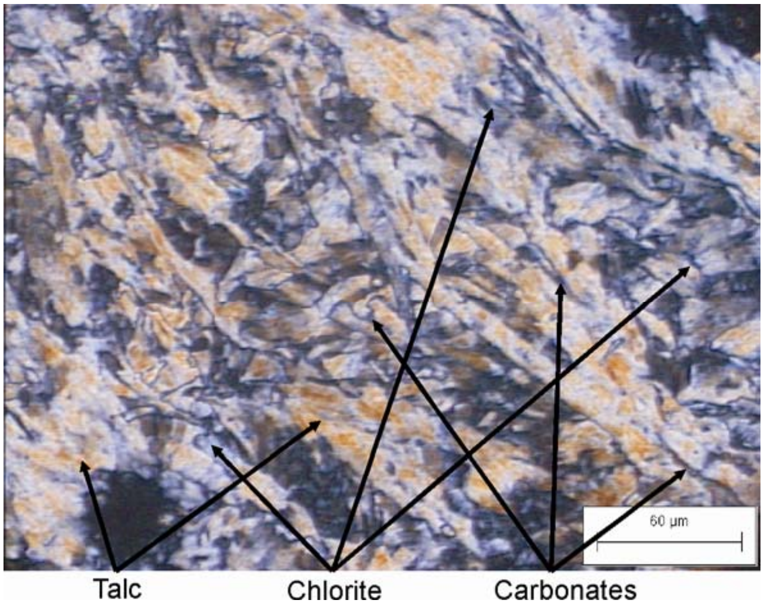

Figure 5

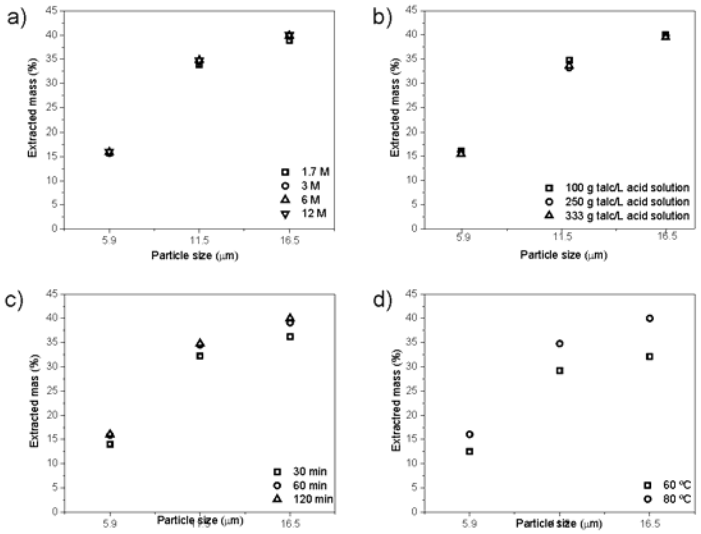
a)
Extracted mass (%)
0
5
10
15
20
25
30
35
40
45
5.9
11.5
16.5
Particle size (μm)
1.7 M
3 M
6 M
12 M
b)
Extracted mass (%)
Particle size (μm)
100 g talc/L acid solution
250 g talc/L acid solution
333 g talc/L acid solution
c)
Extracted mas (%)
Particle size (μm)
30 min
60 min
120 min
d)
Extracted mass (%)
Particle size (μm)
60 ºC
80 ºC

Figure 6

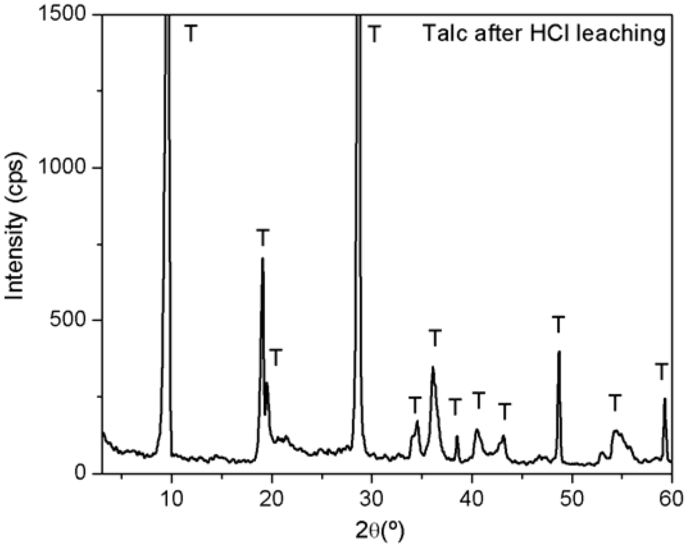
Talc after HCl leaching
Intensity (cps)
2θ(°)
0
500
1000
1500
10
20
30
40
50
60
T

Figure 7

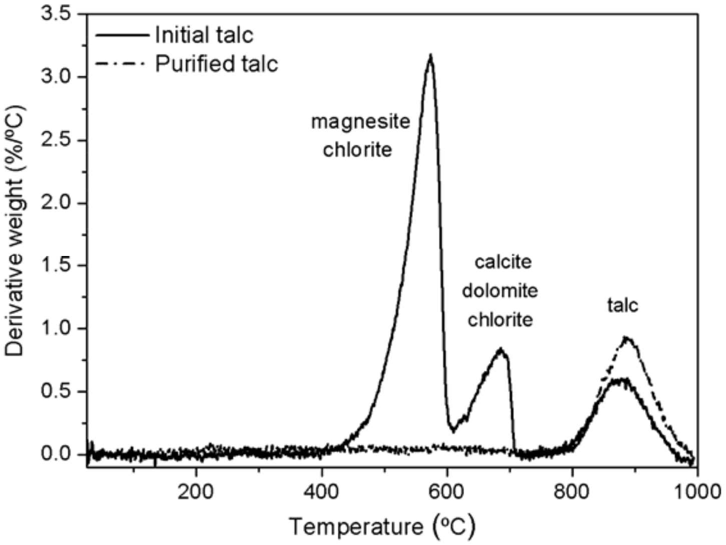

Initial talc
Purified talc
magnesite
chlorite
calcite
dolomite
chlorite
talc
Derivative weight (%/ºC)
0.0
0.5
1.0
1.5
2.0
2.5
3.0
3.5
200
400
600
800
1000
Temperature (ºC)

Figure 8

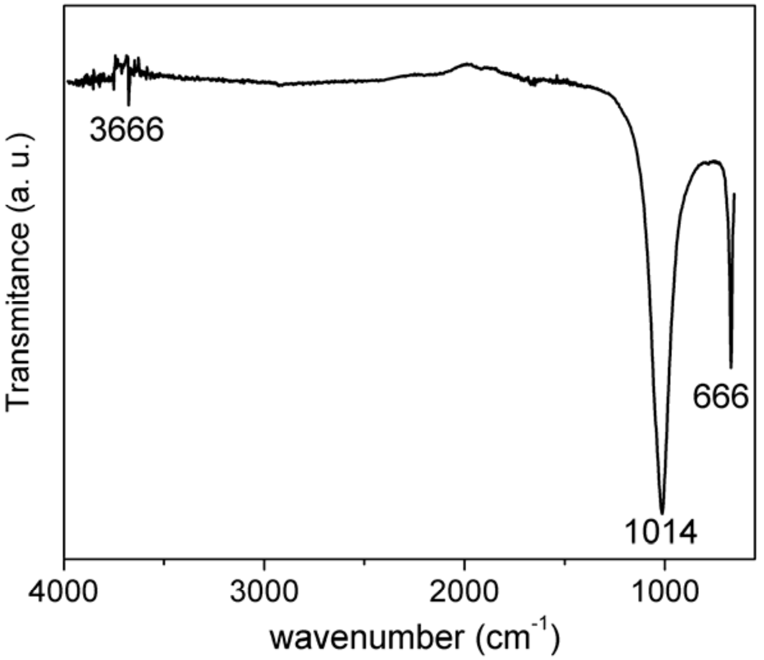
3666
666
1014
Transmitance (a. u.)
4000
3000
2000
1000
wavenumber (cm^{-1})

Figure 9

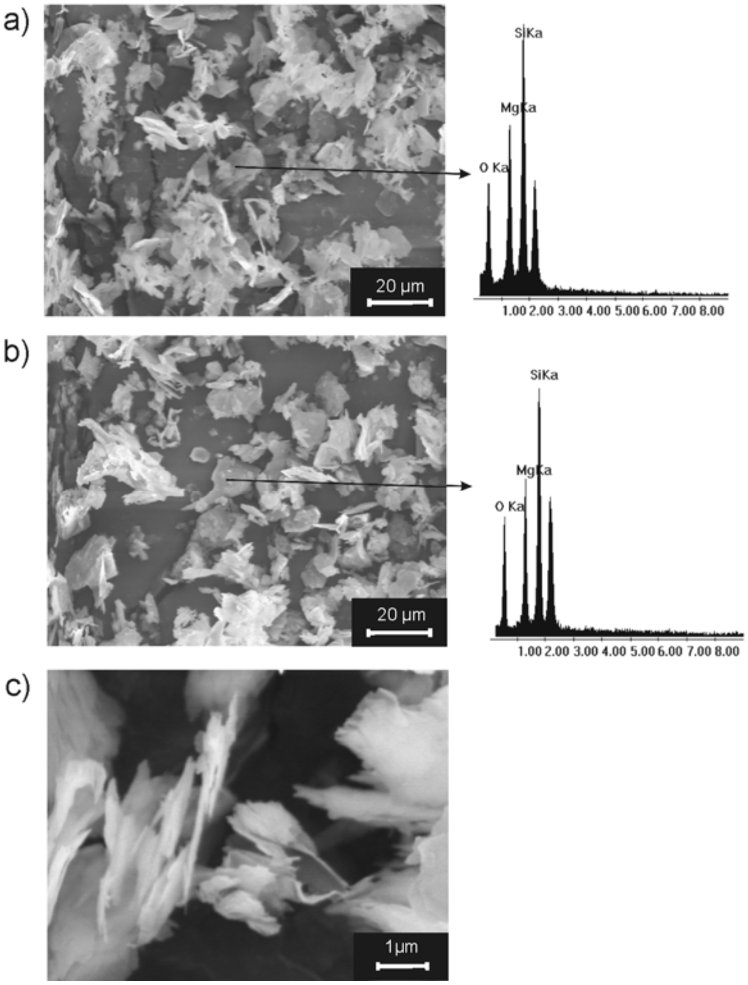
a)
20 µm
SiKa
MgKa
O Ka
1.00 2.00 3.00 4.00 5.00 6.00 7.00 8.00
b)
20 µm
SiKa
MgKa
O Ka
1.00 2.00 3.00 4.00 5.00 6.00 7.00 8.00
c)
1µm

Figure 10